THE JOURNAL OF PHYSICAL CHEMISTRY A
A JOURNAL OF THE AMERICAN CHEMICAL SOCIETY

pubs.acs.org/JPCA

Article

Competing Si_2CH_4–H_2 and $SiCH_2$–SiH_4 Channels in the Bimolecular Reaction of Ground-State Atomic Carbon ($C(^3P_j)$) with Disilane (Si_2H_6, X^1A_{1g}) under Single Collision Conditions

Dababrata Paul,[§] Bing-Jian Sun,[§] Chao He, Zhenghai Yang, Shane J. Goettl, Tao Yang, Bo-Yu Zhang, Agnes H. H. Chang,* and Ralf I. Kaiser*

Cite This: *J. Phys. Chem. A* 2023, 127, 1901–1908

Read Online

ACCESS | Metrics & More | Article Recommendations | Supporting Information

ABSTRACT: The bimolecular gas-phase reaction of ground-state atomic carbon ($C(^3P_j)$) with disilane (Si_2H_6, X^1A_{1g}) was explored under single-collision conditions in a crossed molecular beam machine at a collision energy of 36.6 ± 4.5 kJ mol^{-1}. Two channels were observed: a molecular hydrogen elimination plus Si_2CH_4 (reaction 1) pathway and a silane loss channel along with the formation of $SiCH_2$ (reaction 2), with branching ratios of 20 ± 3 and 80 ± 4%, respectively. Both channels involved indirect scattering dynamics via long-lived Si_2CH_6 reaction intermediate(s); the latter eject molecular hydrogen and silane in "molecular" elimination channels within the rotational plane of the fragmenting intermediate nearly perpendicularly to the total angular momentum vector. These molecular elimination channels are associated with tight exit transition states as reflected in a significant electron rearrangement as visible from the chemical bonding in the light reaction products molecular hydrogen and silane. Once these hydrogenated silicon-carbide clusters are formed within the inner envelope of carbon stars such as of IRC + 10216, the stellar wind can drive both Si_2CH_4 and $SiCH_2$ to the outside sections of the envelope, where they can be photolyzed. This is of particular importance to unravel potential formation pathways to disilicon monocarbide (Si_2C) observed recently in the circumstellar shell of IRC + 10216.

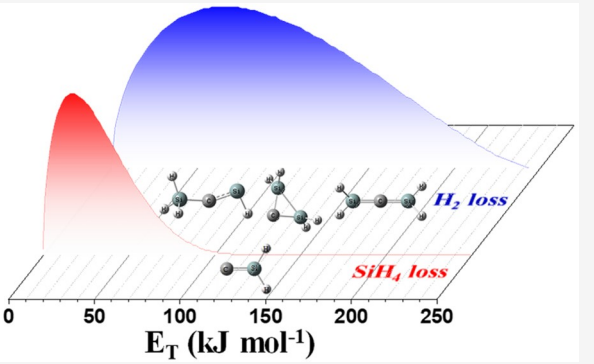

1. INTRODUCTION

Since the very first astronomical detection of silicon dicarbide (c-SiC_2) in the circumstellar envelope (CSE) of the carbon-rich asymptotic giant branch (AGB) star IRC + 10216 in 1984,[1] CSEs have emerged as molecular factories of carbon- and silicon-bearing molecules.[2−7] As of today, 13 molecules containing silicon have been observed in the circumstellar shell of IRC + 10216 (Scheme 1). These organosilicon molecules have received special attention considering their role as fundamental molecular building blocks in the formation of silicon-carbide dust grains in the outflow of CSEs.[8] An emission band close to 11.3 μm (885 cm^{-1}) observed by the infrared astronomical satellite (IRAS) confirms the presence of silicon carbide dust grains[9,10] with up to 90% of the silicon carbide grains extracted from meteorites linked to circumstellar origins.[11,12] The molecular precursors to these grains carry silicon−carbon bond(s) and include, for instance, silicon carbide (SiC),[2] silicon dicarbide (SiC_2),[1] disilicon monocarbide (Si_2C),[6] silicon tricarbide (SiC_3),[4] silicon tetracarbide (SiC_4),[3] and hydrogenated counterparts such as methyl silane (CH_3SiH_3).[7] These building blocks might form close to the central star within a few stellar radii at temperatures ranging from 1000 to 2500 K,[13,14] followed by ejection

Scheme 1. Silicon Containing Molecules Detected in the CSE of IRC + 10216; Silicon, Carbon, Nitrogen, Oxygen, Sulfur, and Hydrogen are Color Coded in Purple, Gray, Blue, Red, Yellow, and White, Respectively

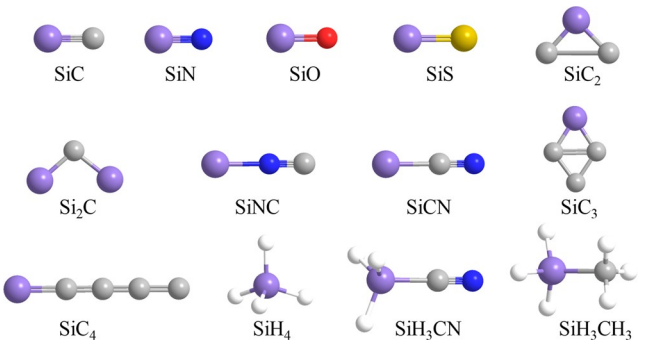

Received: November 30, 2022
Revised: January 30, 2023
Accepted: January 31, 2023
Published: February 15, 2023

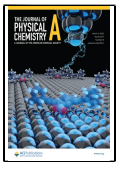

through the stellar wind to the outer envelope, where hydrogenated silicon carbides can be photodissociated to the bare silicon carbon clusters such as the bicyclic silicon tricarbide (c-SiC_3).[15,16]

Considering the importance of silicon carbide grains, it is vital to explore the fundamental reaction mechanisms initiating carbon−silicon bond formation under circumstellar conditions. Both silicon and carbon belong to main group 14 and hence should have similar reactivity according to Langmuir's concept of isovalency.[17,18] However, recent laboratory studies augmented by electronic structure calculations revealed that this simple picture is largely incomplete.[19,20] The simplest hydrocarbon methane (CH_4), for instance, is unreactive toward ground-state atomic carbon ($C(^3P_j)$),[19,21] whereas the reaction with isovalent silane (SiH_4) generates the silylenemethyl ($HCSiH_2$; X^2B_2) radical.[22] Likewise, the chemical bonding of "all carbon" versus "all silicon" species differs dramatically. Disilyne (Si_2H_2), for instance, exhibits a dibridged structure as a global minimum ($Si\mu H_2Si$), whereas acetylene is linear.[23] Disilene (Si_2H_4) exists as a trans-bent molecule with sp^3 hybridized silicon atoms, but the ethylene (C_2H_4) molecule is planar with both carbon atoms sp^2 hybridized.[24,25]

However, whereas an understanding of the chemistry of silane (SiH_4) with carbon-bearing reactants in CSEs is beginning to emerge,[22,26,27] the chemistry of disilane (Si_2H_6) has remained largely unexplored. An elucidation of the reaction dynamics of disilane (Si_2H_6) with ground-state atomic carbon ($C(^3P_j)$) as the simplest "organic" open shell species affords an exceptional opportunity to gauge the activation of disilane through the initial formation of silicon−carbon versus silicon−hydrogen bonds under single collision conditions. This also allows us to contemplate the reaction mechanisms with those on the isovalent disilane (Si_2H_6)−silicon ($Si(^3P_j)$), leading to trisilicontetrahydride (Si_3H_4) via molecular hydrogen elimination through non-adiabatic reaction dynamics.[28] Here, we explored the outcome of the bimolecular reaction of ground-state atomic carbon ($C(^3P_j)$) with disilane (Si_2H_6, X^1A_{1g}) under single collision conditions in the gas phase, exploiting a crossed molecular beam machine. This study revealed two competing channels involving non-adiabatic reaction dynamics: molecular hydrogen (H_2) elimination accompanied by the generation of Si_2CH_4 and silane (SiH_4) plus $SiCH_2$.

2. METHODS

2.1. Experimental Section. The bimolecular reaction of ground-state atomic carbon ($C(^3P_j)$) with disilane (Si_2H_6, X^1A_{1g}) was investigated under single collision conditions utilizing a universal crossed molecular beam machine.[29] In the primary source chamber, the carbon atoms were generated through laser ablation by focusing the fourth harmonic of the Nd:YAG laser output at 266 nm with an energy of 10 mJ $pulse^{-1}$ onto a rotating graphite rod at a repetition rate of 30 Hz.[30] A pulse of helium gas (He, 99.9999%, Gaspro) at 4 atm backing pressure in a pulsed valve was employed to seed the laser-ablated carbon species. The nascent ground-state atomic carbon ($C(^3P_j)$) beam was then skimmed by a conical skimmer with an opening of 1 mm and traveled to the interaction region after velocity selection by a four-slotted chopper wheel rotating at 120 Hz. A photodiode mounted at the chopper wheel acted as a "time zero" of the experiments. The pulse valve delay between the photo diode and the laser trigger was optimized to 1894 μs, resulting in a peak velocity of ground-state carbon atoms, Vp, of 2595 ± 161 ms^{-1} and a speed ratio, S, of 2.1 ± 0.3 (Table 1). In the secondary source chamber, a pulsed, supersonic beam of disilane (99.998%, Voltaix) was generated with the peak velocity Vp of 742 ± 35 ms^{-1} and the speed ratio S of 7.2 ± 0.7 at a backing pressure of 500 Torr; this beam crossed the primary carbon atom beam in the interaction region perpendicularly resulting in a collision energy, E_C, of 36.6 ± 4.5 kJ mol^{-1} and a center of mass angle, θ_{CM}, of 56.6 ± 0.4°. In the laser ablation source,[29,31−33] the delay times, laser power, and laser focus were optimized to generate a beam with 95% atomic carbon; dicarbon[30,34−36] and tricarbon could be minimized to 5%. The center of mass angles of the dicarbon−disilane and tricarbon−disilane were 37.2 ± 0.4 and 27 ± 0.4°, respectively. A potential reactive scattering signal was searched for the dicarbon−disilane and tricarbon−disilane systems, but no ion counts higher than 74 were observed. Therefore, although the primary molecular beam contains dicarbon and tricarbon, they do not interfere under our experimental conditions.

Table 1. Peak Velocities (Vp) and Speed Ratios (S) of the Carbon (C) and Disilane (Si_2H_6) Beams along with the Corresponding Collision Energy (E_C) and CM Angle (θ_{CM})

beam	Vp (ms^{-1})	S	E_C (kJ mol^{-1})	θ_{CM} (deg)
$C(^3P_j)$	2595 ± 161	2.1 ± 0.3	36.6 ± 4.5	56.6 ± 0.4
$Si_2H_6(X^1A_1)$	742 ± 35	7.2 ± 0.7		

The scattered products entered a triply differentially pumped universal mass spectrometric detector operating in the time-of-flight (TOF) mode. Here, the neutral reaction products were ionized by electron impact (80 eV) and then filtered according to their mass-to-charge (m/z) ratio using a quadrupole mass spectrometer (QMS) operating in the TOF mode. The detection apparatus was housed in a differentially pumped, rotatable chamber that allowed for the measurement of angularly resolved TOF spectra in the plane of the reactant beams. The laboratory data were converted to the center-of-mass (CM) reference frame through a forward-convolution routine that relies on user-defined CM translational energy $P(E_T)$ and angular $T(\theta)$ flux distributions; these are varied iteratively until a best fit of the experimental data set is obtained.[37,38] The product flux contour map is defined by the CM functions and shows the differential reactive cross-section, $I(u,\theta) \sim P(u) \times T(\theta)$, as a function of intensity with respect to the angle θ and the CM velocity u.[39] Errors of the $P(E_T)$ and $T(\theta)$ functions were determined within the 1σ limits of the corresponding laboratory angular distributions and beam parameters such as beam velocities and speed ratios.

2.2. Computational Details. The geometries of possible isomers of the singlet and triplet Si_2CH_4 and doublet Si_2CH_5 products for the reaction of carbon ($C(^3P_j)$) with disilane (Si_2H_6, X^1A_{1g}) were optimized with B3LYP[40,41]/cc-pVTZ calculations. Their corresponding CCSD(T)[42,43]/CBS (complete basis set limits[44]) energies are then obtained by extrapolating the CCSD(T)/cc-pVDZ, CCSD(T)/cc-pVTZ, and CCSD(T)/cc-pVQZ energies, with B3LYP/cc-pVTZ zero-point energy corrections. The accuracy of these CCSD(T)/CBS energies is expected to be within 8 kJ mol^{-1}.[45] GAUSSIAN16 programs[46] are facilitated in the electronic structure calculations.

3. RESULTS AND DISCUSSION

3.1. Laboratory Data. Reactive scattering signal was recorded at m/z = 74 ($^{28}Si^{29}SiH_5{}^{12}C/^{28}Si^{28}SiH_5{}^{13}C/^{28}$

https://doi.org/10.1021/acs.jpca.2c08417
J. Phys. Chem. A 2023, 127, 1901−1908

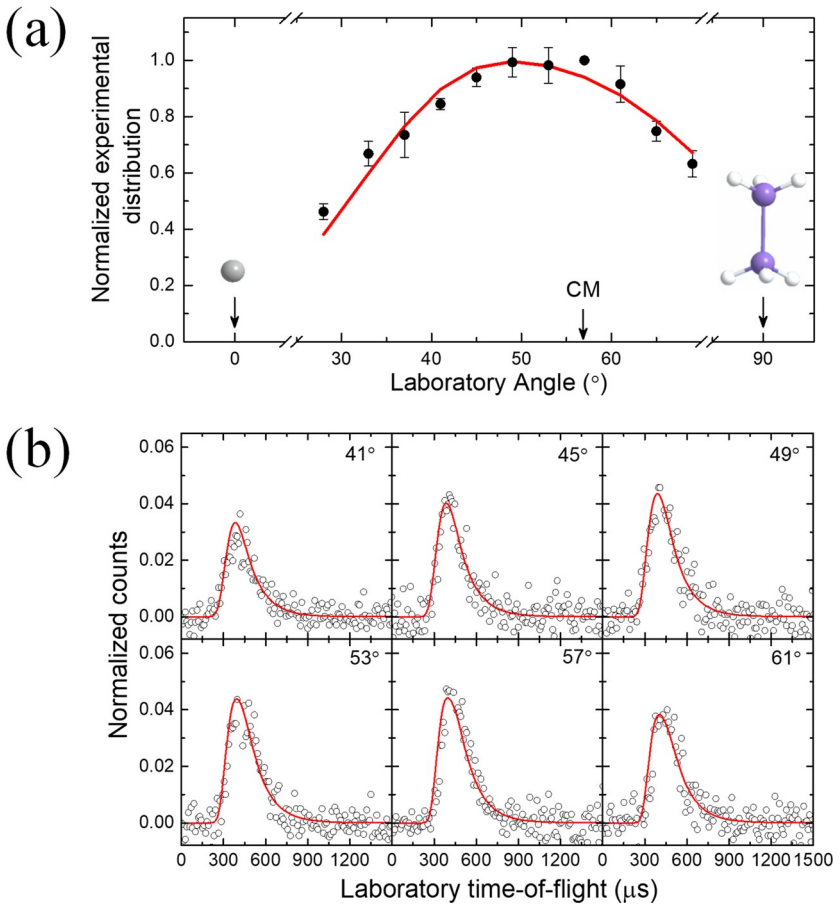

Figure 1. Laboratory angular distribution of the Si_2CH_4 product (72 amu) recorded at m/z = 71 ($Si_2CH_3^+$) collected in the reaction of atomic carbon with disilane together with selected TOF spectra. Open circles indicate experimental data, and the solid red line the calculated distribution with the best-fit CM functions. CM designates the CM angle.

$Si^{30}SiH_4{}^{12}C/{}^{29}Si^{29}SiH_4{}^{12}C/{}^{28}Si^{29}SiH_4{}^{13}C/{}^{29}Si^{30}SiH_3{}^{12}C/{}^{28}Si^{30}SiH_3{}^{13}C/{}^{29}Si^{29}SiH_3{}^{13}C/{}^{30}Si^{30}SiH_2{}^{12}C/{}^{29}Si^{30}SiH_2{}^{13}C/{}^{30}Si^{30}SiH{}^{13}C$), m/z = 73 ($^{28}Si^{28}SiH_5{}^{12}C/{}^{28}Si^{29}SiH_4{}^{12}C/{}^{28}Si^{28}SiH_4{}^{13}C/{}^{28}Si^{30}SiH_3{}^{12}C/{}^{29}Si^{29}SiH_3{}^{12}C/{}^{28}Si^{29}SiH_3{}^{13}C/{}^{29}Si^{30}SiH_2{}^{12}C/{}^{28}Si^{30}SiH_2{}^{13}C/{}^{29}Si^{29}SiH_2{}^{13}C/{}^{30}Si^{30}SiH{}^{12}C/{}^{29}Si^{30}SiH{}^{13}C$), m/z = 72 ($^{28}Si^{28}SiH_4{}^{12}C/{}^{29}Si^{28}SiH_3{}^{12}C/{}^{28}Si^{28}SiH_3{}^{13}C/{}^{30}Si^{28}SiH_2{}^{12}C/{}^{29}Si^{29}SiH_2{}^{12}C/{}^{28}Si^{29}SiH_2{}^{13}C/{}^{29}Si^{30}SiH{}^{12}C/{}^{28}Si^{30}SiH{}^{13}C/{}^{29}Si^{29}SiH{}^{13}C$), m/z = 71 ($^{28}Si^{28}SiH_3{}^{12}C/{}^{29}Si^{28}SiH_2{}^{12}C/{}^{28}Si^{28}SiH_2{}^{13}C/{}^{30}Si^{28}SiH{}^{12}C/{}^{29}Si^{29}SiH{}^{12}C/{}^{28}Si^{29}SiH{}^{13}C$), and m/z = 42 ($^{28}SiH_2{}^{12}C/{}^{29}SiH{}^{12}C/{}^{28}SiH{}^{13}C/{}^{29}Si{}^{13}C/{}^{30}Si{}^{12}C$) (Table S1), taking into account the natural isotope abundances of silicon [^{28}Si (92.2%), ^{29}Si (4.7%), ^{30}Si (3.1%)], and carbon [^{12}C (98.9%), ^{13}C (1.1%)]. Hence, the signal at m/z = 74 to 71 can be attributed to the atomic and/or molecular hydrogen loss channels along with dissociative ionization of the primary reaction products in the electron impact ionizer. After scaling, the TOF spectra collected from m/z = 73 to 71 reveal identical patterns (Figure S1). The ratio of the integrated ion signal of m/z = 72 and 73 of 7.2 ± 1.0 suggests that m/z = 73 originates from ^{29}Si and ^{13}C-substituted $^{28}Si^{28}SiH_4{}^{12}C$ (72 amu), with the latter formed through molecular hydrogen loss. However, the signal at m/z = 74 is very weak; based on the limited signal-to-noise ratio, there is no substantiative evidence of atomic hydrogen loss under the current experimental conditions. Note that based on the naturally occurring isotope fractions, a ratio of 6.3 ($S_{m/z=72}/S_{m/z=73}$ = 99.9/15.9 = 6.3) is expected. Furthermore, the overlapping shapes of the TOFs propose that the signal at m/z = 71 originates from dissociative ionization of the Si_2CH_4 neutral in the electron impact ionizer. Most importantly, the TOF spectra recorded at m/z = 42 do not overlap with those collected at higher mass-to-charge ratios (Figure S2). This significant finding indicates that ion counts at m/z = 42 originate at least partially from reactive scattering signals and hence result in the formation of a molecule with the formula $^{28}Si^{12}CH_2$ (42 amu; hereafter $SiCH_2$) along with the loss of silane (SiH_4; 32 amu). Therefore, the laboratory data alone provide compelling evidence on the existence of two channels: Si_2CH_4 plus molecular hydrogen (reaction 1) and $SiCH_2$ plus silane (reaction 2).

$$C(^3P_j) + Si_2H_6 \rightarrow Si_2CH_4 + H_2 \quad (1)$$

$$C(^3P_j) + Si_2H_6 \rightarrow SiCH_2 + SiH_4 \quad (2)$$

It is noted that compared to m/z = 72, the signal-to-noise (S/N) ratio at m/z = 71 is enhanced by a factor of 2.3; thus, the full laboratory angular distribution was extracted at m/z = 71. The TOF spectra and the corresponding laboratory angular distributions derived from the ion counts at m/z = 71 and 42 are displayed in Figures 1 and 2, respectively. The TOF spectra for both channels are very broad, spanning more than 500 μs. The resulting laboratory angular distributions, which cover more than 50° within the scattering plane as defined by both beams, are distinct in shape. These findings also point to distinct scattering dynamics and exit channels involving the CSi_2H_6 collision complex(es). To account for the broad and

https://doi.org/10.1021/acs.jpca.2c08417
J. Phys. Chem. A 2023, 127, 1901−1908

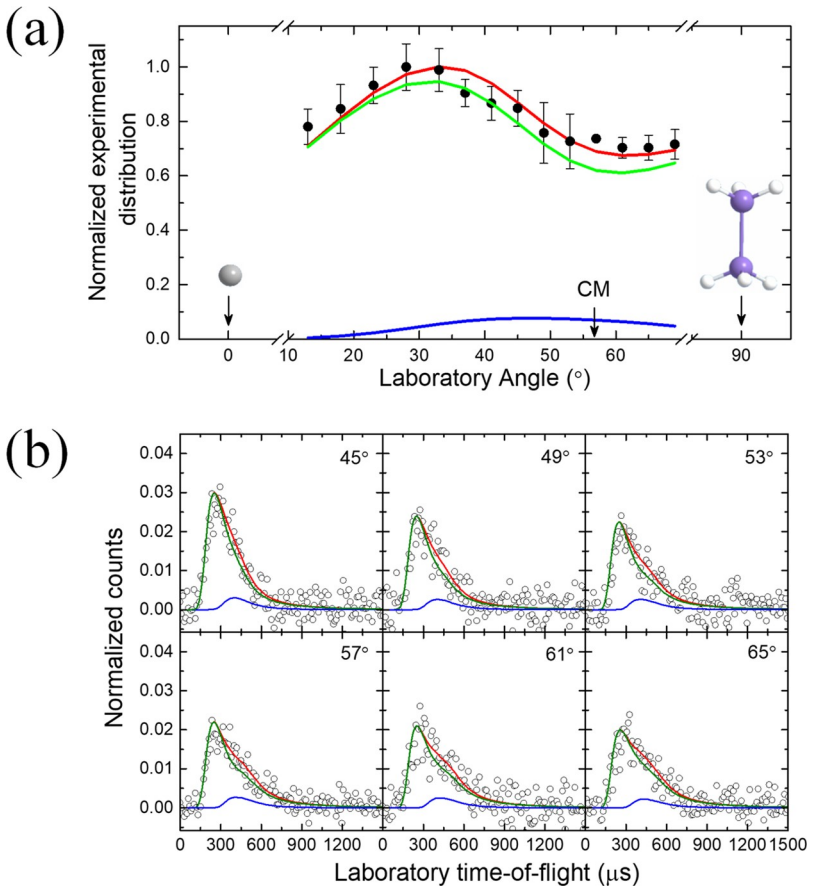

Figure 2. Laboratory angular distribution of m/z = 42 ($SiCH_2^+$) recorded for the reaction of atomic carbon with disilane together with selected TOF spectra. Open circles indicate experimental data, and the solid red line the overall calculated distribution with the best-fit CM functions. CM designates the CM angle. The two-channel fit represents the dissociative electron impact ionization of the heavy product (Si_2CH_4) in reaction 1 to m/z = 42 (blue line) and the ionized $SiCH_2$ product for reaction 2 (green line).

asymmetric distribution of $SiCH_2$ formation, a channel arising from the dissociative electron impact ionization of the heavy product Si_2CH_4 in the electron impact ionizer to $SiCH_2^+$ was required. This distribution yields a maximum at 50 ± 0.5°, which is close to the CM angle. However, at lower laboratory angles, a single channel involving reaction 2 is sufficient to fit the reactive scattering data.

3.2. CM Data. To investigate the underlying mechanisms of reactions 1 and 2, we inspect the CM translational energy distributions, $P(E_T)$, and angular flux distributions, $T(\theta)$ (Figure 3). The high-energy cutoff of the $P(E_T)$ can be determined for those molecules born without internal excitation through energy conservation via $E_T^{Max} = E_C - \Delta_r G$, where E_C and $\Delta_r G$ represent the collision energy and the reaction energy, respectively. The CM translational energy distribution of the Si_2CH_4 pathway (reaction 1) via molecular hydrogen (H_2) loss (Figure 3b) is broader compared to $SiCH_2$ formation via silane (SiH_4) elimination (Figure 3a); these yield maximum kinetic energy releases of 242 ± 12 kJ mol^{-1} (reaction 1) and 109 ± 10 kJ mol^{-1} (reaction 2), respectively. A subtraction of the collision energy, 36.6 ± 4.5 kJ mol^{-1}, reveals that the reactions are exoergic by 205 ± 12 and 72 ± 10 kJ mol^{-1}, respectively. The $P(E_T)$s of these two channels peak at 66 ± 3 and 36 ± 3 kJ mol^{-1}, indicating the presence of tight transition state(s) in the exit channel(s). Furthermore, these distributions account for an average of 94 ± 5 and 32 ± 3 kJ mol^{-1} translational energies. With respect to the CM angular distributions, $T(\theta)$, both distributions reveal forward−backward symmetries with coplanar scattering associated with a distribution minimum at 90° for both channels. These findings suggest the involvement of indirect scattering dynamics with CSi_2H_6 collision complex(es) having a lifetime longer than their rotational periods prior to dissociation to Si_2CH_4 plus molecular hydrogen (H_2) and $CSiH_2$ plus silane (SiH_4). These findings are also compiled in the flux contour maps (Figure 3e,f), which depict the flux intensity of reactively scattering products as a function of the scattering angle (θ) and product velocity (u), providing detailed angular information about the reactive scattering process. Overall, these two channels result in a branching ratio of 20 ± 3 and 80 ± 4%, for the molecular hydrogen and silane loss channels through reactions 1 and 2, respectively.[47,48]

3.3. Electronic Structure Calculations. *3.3.1. Molecular Hydrogen Loss Channel.* To explore possible product isomers formed in the reaction of atomic carbon with disilane in reaction 1, we explore computationally the reaction energies to form various Si_2CH_4 isomers on the triplet and singlet surfaces. Our investigations indicate the existence of 13 triplet and 10 singlet Si_2CH_4 isomers displaying Si−Si−C, Si−C−Si, and cyclic Si−C−Si moieties (Figure 4, Table S2). On the triplet surface, reaction exoergicities range from 75 to 353 kJ mol^{-1}, while the singlet surface reveals reaction exoergicities from 311 to 456 kJ mol^{-1}; these reaction energies are accurate within ±8 kJ mol^{-1}. How do these reaction energies correlate with the experimentally derived reaction energy of 205 ± kJ mol^{-1}? On the triplet surface, this energy could correlate well with the

https://doi.org/10.1021/acs.jpca.2c08417
J. Phys. Chem. A 2023, 127, 1901−1908

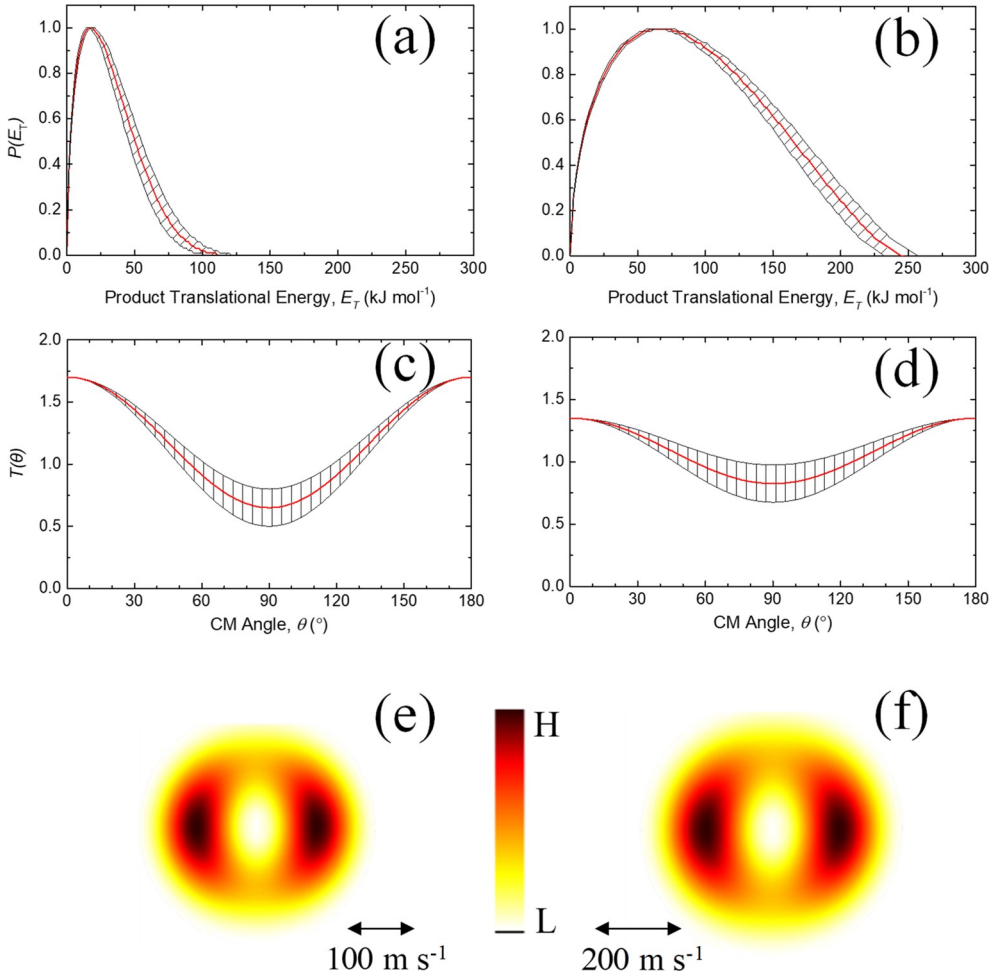

Figure 3. CM translational energy flux distributions (a,b) and angular distributions (c,d) along with the flux contour map (e,f), leading to the formation of $SiCH_2^+$ (m/z = 42) and $Si_2CH_4^+$ (m/z = 72) in the reaction of atomic carbon with disilane. Hatched areas indicate the acceptable upper and lower error limits of the fits. The solid red lines define the best-fit function to replicate the laboratory data as shown in Figures 1 and 2. The flux contour maps represent the flux intensity of the reactive scattering products as a function of the CM scattering angle (θ) and product velocity (u). The color bar indicates the flux gradient from low (L) intensity to high (H) intensity. Panels (a,c,e) reflect reaction 2 and panels (b,d,f) reaction 1.

formation of ^{3}p3 to ^{3}p5. These structures hold one common structural moiety: the Si−C−Si unit. This could indicate that the carbon atom reacts preferentially with the silicon atom, followed by cyclization and/or ring opening and molecular hydrogen loss on the triplet surface. Alternatively, on the singlet surface, none of the computed reaction energies can match the experimentally determined value, with the latter being too low by at least 106 kJ mol^{-1}. However, this discrepancy could be accounted for if, on the singlet surface, the Si_2CH_4 products are highly vibrationally excited. This in turn could result in significantly less energy released in the translational degrees of freedom as exposed recently for the dicarbon (C_2)−silane (SiH_4)[49] and methylidyne (CH)−dimethylacetylene (CH_3CCCH_3) systems.[50]

3.3.2. Silane Loss Channel. The silane loss channel results in the formation of the heavy $SiCH_2$ (42 amu) co-product. Extracting enthalpies of formation of three $SiCH_2$ isomers,[22] the reaction exoergicities to form the three isomers are 428 kJ mol^{-1} (silylidene, H_2CSi), 288 kJ mol^{-1} (silaacetylene, HCSiH), and 80 kJ mol^{-1} (silylenecarbene, H_2SiC), respectively. The reaction exoergicities leading to their triplet states are 263 kJ mol^{-1} (triplet silylidene, H_2CSi), 174 kJ mol^{-1} (triplet silaacetylene, HCSiH), and 66 kJ mol^{-1} (silylenecarbene, H_2SiC), respectively. Errors of these data are ±8 kJ mol^{-1}.[22] On the singlet surface, all reaction energies are higher than the experimentally derived value of 72 ± 10 kJ mol^{-1}. This suggests that if singlet $SiCH_2$ (42 amu) is formed, these molecules are highly vibrationally excited, thus shifting the maximum translational energy releases to lower values. This conclusion also holds if triplet silylidene (H_2CSi) or triplet silaacetylene (HCSiH) are the reaction products. Note that, in principle, the computed energy of 66 kJ mol^{-1} for silylenecarbene (H_2SiC) would fit nicely with the experimentally derived values. Overall, the elucidation of the isomers requires not only a computation of the complete potential energy surface (PES) on the triplet and singlet manifolds but also the identification of conical intersection for intersystem crossing (ISC). Furthermore, quasiclassical trajectory calculations are imperative to predict the center of mass functions and to compare those for distinct exit channels with the experimental findings. This endeavor is beyond the scope of this paper.

4. CONCLUSIONS

In the present study, the elementary reaction between the ground-state atomic carbon ($C(^3P_j)$) and disilane (Si_2H_6, X^1A_{1g}) was explored using the crossed molecular beam apparatus at a collision energy of 36.6 ± 4.5 kJ mol^{-1}. At this collision energy,

https://doi.org/10.1021/acs.jpca.2c08417
J. Phys. Chem. A 2023, 127, 1901−1908

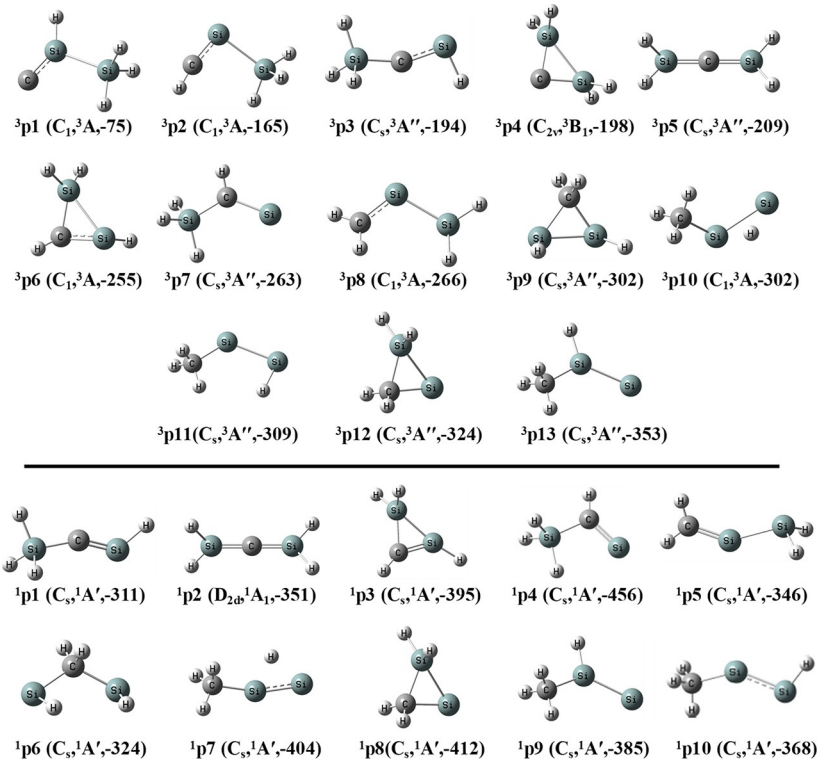

Figure 4. B3LYP/cc-pVTZ-optimized geometries of triplet and singlet Si_2CH_4 isomers along with their CCSD(T)/CBS relative energies in kJ mol^{-1} with respect to the separated reactants.

the reactions leading to the formation of Si_2CH_4 and $SiCH_2$ were attributed to two competing exit channels via molecular hydrogen and silane elimination, respectively, with branching ratios of 20 ± 3 and 80 ± 4%. Both channels involved indirect scattering dynamics via long-lived Si_2CH_6 reaction intermediates which lose molecular hydrogen and also silane in "molecular" elimination channels within the rotational plane of the fragmenting intermediate nearly perpendicularly to the total angular momentum vector. Upon formation of these hydrogenated silicon-carbide clusters within the inner envelope of carbon stars such as of IRC+10216, the stellar wind can eject both Si_2CH_4 and $SiCH_2$ outside, where they can be photolyzed.[51] This is of particular importance to unravel potential formation pathways to disilicon monocarbide (Si_2C).[6]

■ ASSOCIATED CONTENT

Supporting Information

The Supporting Information is available free of charge at https://pubs.acs.org/doi/10.1021/acs.jpca.2c08417.

TOF spectra at different mass-to-charge ratios, natural isotopic abundance of the products, B3LYP/cc-pVTZ-optimized Cartesian coordinates, vibrational frequencies, and infrared intensities of singlet and triplet Si_2CH_4 and doublet Si_2CH_5 isomers (PDF)

■ AUTHOR INFORMATION

Corresponding Authors

Agnes H. H. Chang − *Department of Chemistry, National Dong Hwa University, Shoufeng, Hualien 974, Taiwan*; Email: hhchang@gms.ndhu.edu.tw

Ralf I. Kaiser − *Department of Chemistry, University of Hawai'i at Manoa, Honolulu, Hawaii 96822, United States*; orcid.org/0000-0002-7233-7206; Email: ralfk@hawaii.edu

Authors

Dababrata Paul − *Department of Chemistry, University of Hawai'i at Manoa, Honolulu, Hawaii 96822, United States*

Bing-Jian Sun − *Department of Chemistry, National Dong Hwa University, Shoufeng, Hualien 974, Taiwan*

Chao He − *Department of Chemistry, University of Hawai'i at Manoa, Honolulu, Hawaii 96822, United States*

Zhenghai Yang − *Department of Chemistry, University of Hawai'i at Manoa, Honolulu, Hawaii 96822, United States*

Shane J. Goettl − *Department of Chemistry, University of Hawai'i at Manoa, Honolulu, Hawaii 96822, United States*

Tao Yang − *Department of Chemistry, University of Hawai'i at Manoa, Honolulu, Hawaii 96822, United States*

Bo-Yu Zhang − *Department of Chemistry, National Dong Hwa University, Shoufeng, Hualien 974, Taiwan*

Complete contact information is available at: https://pubs.acs.org/10.1021/acs.jpca.2c08417

Author Contributions

[§]D.P. and B.-J.S. contributed equally.

Notes

The authors declare no competing financial interest.

■ ACKNOWLEDGMENTS

This work was supported by the U.S. National Science Foundation, Division of Chemistry (CHEM 1853541), to the University of Hawaii at Manoa. B.-J.S., B.-Y.Z., and A.H.H.C. thank the National Center for High-performance Computer in Taiwan for providing the computer resources.

REFERENCES

(1) Thaddeus, P.; Cummins, S. E.; Linke, R. A. Identification of the SiCC radical toward IC +10216: The first molecular ring in an astronomical source. *Astrophys. J.* **1984**, *283*, L45.

(2) Cernicharo, J.; Gottlieb, C. A.; Guelin, M.; Thaddeus, P.; Vrtilek, J. M. Astonomical and laboratory detection of the SiC radical. *Astrophys. J.* **1989**, *341*, L25.

(3) Ohishi, M.; Kaifu, N.; Kawaguchi, K.; Murakami, A.; Saito, S.; Yamamoto, S.; Ishikawa, S.-I.; Fujita, Y.; Shiratori, Y.; Irvine, W. M. Detection of a new circumstellar carbon chain molecule C_4Si. *Astrophys. J.* **1989**, *345*, L83.

(4) Apponi, A. J.; McCarthy, M. C.; Gottlieb, C. A.; Thaddeus, P. Astronomical detection of rhomboidal SiC_3. *Astrophys. J.* **1999**, *516*, L103.

(5) Guélin, M.; Muller, S.; Cernicharo, J.; Apponi, A. J.; McCarthy, M. C.; Gottlieb, C. A.; Thaddeus, P. Astronomical detection of the free radical SiCN. *Astron. Astrophys.* **2000**, *363*, L9−L12.

(6) Cernicharo, J.; McCarthy, M. C.; Gottlieb, C. A.; Agúndez, M.; Prieto, L. V.; Baraban, J. H.; Changala, P. B.; Guélin, M.; Kahane, C.; Drumel, M. A. M.; et al. Discovery of SiCSi in IRC+10216: A missing link between gas and dust carriers of Si−C bonds. *Astrophys. J.* **2015**, *806*, L3.

(7) Cernicharo, J.; Agúndez, M.; Velilla Prieto, L.; Guélin, M.; Pardo, J. R.; Kahane, C.; Marka, C.; Kramer, C.; Navarro, S.; Quintana-Lacaci, G.; et al. Discovery of methyl silane and confirmation of silyl cyanide in IRC +10216. *Astron. Astrophys.* **2017**, *606*, L5.

(8) Velilla-Prieto, L.; Cernicharo, J.; Agúndez, M.; Fonfría, J. P.; Castro-Carrizo, A.; Quintana-Lacaci, G.; Marcelino, N.; McCarthy, M. C.; Gottlieb, C. A.; Sánchez Contreras, C.; et al. Circumstellar chemistry of Si-C bearing molecules in the C-rich AGB star IRC +10216. *Proc. Int. Astron. Union* **2018**, *14*, 535−537.

(9) Yang, X.; Chen, P.; He, J. Molecular and dust features of 29 SiC carbon AGB stars. *Astron. Astrophys.* **2004**, *414*, 1049−1063.

(10) Treffers, R.; Cohen, M. High-resolution spectra of cool stars in the 10- and 20-micron regions. *Astrophys. J.* **1974**, *188*, 545−552.

(11) Davis, A. M. Stardust in meteorites. *Proc. Natl. Acad. Sci. U.S.A.* **2011**, *108*, 19142−19146.

(12) Zinner, E.; Nittler, L. R.; Gallino, R.; Karakas, A. I.; Lugaro, M.; Straniero, O.; Lattanzio, J. C. Silicon and carbon isotopic ratios in AGB stars: SiC grain data, models, and the galactic evolution of the Si isotopes. *Astrophys. J.* **2006**, *650*, 350−373.

(13) De Beck, E. D. B. E.; Lombaert, R.; Agúndez, M.; Daniel, F.; Decin, L.; Cernicharo, J.; Müller, H. S. P.; Min, M.; Royer, P.; Vandenbussche, B.; et al. On the physical structure of IRC + 10216-ground-based and Herschel observations of CO and C_2H. *Astron. Astrophys.* **2012**, *539*, A108.

(14) Men'shchikov, A. B.; Balega, Y. Y.; Blöcker, T.; Osterbart, R.; Weigelt, G.. In *Post-AGB Objects As A Phase Of Stellar Evolution: Proceedings of the Toruń Workshop Held July 5−7, 2000*; Szczerba, R., Górny, S. K., Eds.; Springer Netherlands: Dordrecht, 2001; pp 343−350.

(15) Agúndez, M.; Fonfría, M.; Cernicharo, J. P.; Kahane, J.; Daniel, C.; Guélin, F.; Guélin, M. Molecular abundances in the inner layers of IRC +10216. *Astron. Astrophys.* **2012**, *543*, A48.

(16) Willacy, K.; Cherchneff, I. Silicon and sulphur chemistry in the inner wind of IRC+10216. *Astron. Astrophys.* **1998**, *330*, 676−684.

(17) Langmuir, I. The arrangement of electrons in atoms and molecules. *J. Am. Chem. Soc.* **1919**, *41*, 868−934.

(18) Langmuir, I. Isomorphism, isosterism and covalence. *J. Am. Chem. Soc.* **1919**, *41*, 1543−1559.

(19) Sakai, S.; Deisz, J.; Gordon, M. S. Theoretical studies of the insertion reactions of atomic carbon and silicon into methane and silane. *J. Phys. Chem.* **1989**, *93*, 1888−1893.

(20) Braun, W.; Bass, A. M.; Davis, D. D.; Simmons, J. D.; Porter, G.; Lighthill, M. J. Flash photolysis of carbon suboxide: absolute rate constants for reactions of $C(^3P)$ and $C(^1D)$ with H_2, N_2, CO, NO, O_2 and CH_4. *Proc. R. Soc. London, Ser. A* **1969**, *312*, 417−434.

(21) Kim, G.-S.; Nguyen, T. L.; Mebel, A. M.; Lin, S. H.; Nguyen, M. T. Ab initio/RRKM study of the potential energy surface of triplet ethylene and product branching ratios of the $C(^3P) + CH_4$ reaction. *J. Phys. Chem. A* **2003**, *107*, 1788−1796.

(22) He, C.; Thomas, A. M.; Dangi, B. B.; Yang, T.; Kaiser, R. I.; Lee, H. C.; Sun, B. J.; Chang, A. H. H. Formation of the elusive silylenemethyl radical ($HCSiH_2$; X^2B_2) via the unimolecular decomposition of triplet silaethylene (H_2CSiH_2; a^3A''). *J. Phys. Chem. A* **2022**, *126*, 3347−3357.

(23) Guidez, E. B.; Gordon, M. S.; Ruedenberg, K. Why is Si_2H_2 not linear? An intrinsic quasi-atomic bonding analysis. *J. Am. Chem. Soc.* **2020**, *142*, 13729−13742.

(24) Nori-Shargh, D.; Mousavi, S. N.; Boggs, J. E. Pseudo Jahn-Teller effect and natural bond orbital analysis of structural properties of tetrahydridodimetallenes M_2H_4, (M = Si, Ge, and Sn). *J. Phys. Chem. A* **2013**, *117*, 1621−1631.

(25) Trinquier, G. Double bonds and bridged structures in the heavier analogs of ethylene. *J. Am. Chem. Soc.* **1990**, *112*, 2130−2137.

(26) Yang, Z.; He, C.; Goettl, S. J.; Paul, D.; Kaiser, R. I.; Silva, M. X.; Galvão, B. R. L. Gas-phase preparation of silyl cyanide (SiH_3CN) via a radical substitution mechanism. *J. Am. Chem. Soc.* **2022**, *144*, 8649−8657.

(27) Lucas, M.; Thomas, A. M.; Yang, T.; Kaiser, R. I.; Mebel, A. M.; Hait, D.; Head-Gordon, M. Bimolecular reaction dynamics in the phenyl-silane system: Exploring the prototype of a radical substitution mechanism. *J. Phys. Chem. Lett.* **2018**, *9*, 5135−5142.

(28) Yang, T.; Dangi, B. B.; Thomas, A. M.; Kaiser, R. I.; Sun, B.-J.; Staś, M.; Chang, A. H. H. Gas-phase synthesis of the elusive trisilicontetrahydride species (Si_3H_4). *J. Phys. Chem. Lett.* **2017**, *8*, 131−136.

(29) Guo, Y.; Gu, X.; Kawamura, E.; Kaiser, R. I. Design of a modular and versatile interlock system for ultrahigh vacuum machines: A crossed molecular beam setup as a case study. *Rev. Sci. Instrum.* **2006**, *77*, 034701.

(30) Gu, X.; Guo, Y.; Kawamura, E.; Kaiser, R. I. Characteristics and diagnostics of an ultrahigh vacuum compatible laser ablation source for crossed molecular beam experiments. *J. Vac. Sci. Technol., A* **2006**, *24*, 505−511.

(31) Kaiser, R. I.; Lee, Y. T.; Suits, A. G. Crossed-beam reaction of $C(^3P_j)$ with $C_2H_2(^1\Sigma_g^+)$: Observation of tricarbon-hydride C_3H. *J. Chem. Phys.* **1995**, *103*, 10395−10398.

(32) Kaiser, R. I.; Stranges, D.; Lee, Y. T.; Suits, A. G. Neutral-Neutral Reactions in the Interstellar Medium. I. Formation of Carbon Hydride Radicals via Reaction of Carbon Atoms with Unsaturated Hydrocarbons. *Astrophys. J.* **1997**, *477*, 982.

(33) Kaiser, R. I.; Sun, W.; Suits, A. G.; Lee, Y. T. Crossed beam reaction of atomic carbon, $C(^3P_j)$, with the propargyl radical, $C_3H_3(X^2B_2)$: Observation of diacetylene, $C_4H_2(X^1\Sigma_g^+)$. *J. Chem. Phys.* **1997**, *107*, 8713−8716.

(34) Karni, M.; Apeloig, Y.; Schröder, D.; Zummack, W.; Rabezzana, R.; Schwarz, H. HCSiF and HCSiCl: the first detection of molecules with formal C≡Si triple bonds. *Angew. Chem., Int. Ed.* **1999**, *38*, 331−335.

(35) Balucani, N.; Mebel, A. M.; Lee, Y. T.; Kaiser, R. I. A combined crossed molecular beam and ab initio study of the reactions $C_2(X^1\Sigma_g^+, a^3\Pi_u) + C_2H_4 \rightarrow n\text{-}C_4H_3(X^2A') + H(^2S_{1/2})$. *J. Phys. Chem. A* **2001**, *105*, 9813−9818.

(36) Kaiser, R. I.; Balucani, N.; Charkin, D. O.; Mebel, A. M. A crossed beam and ab initio study of the $C_2(X^1\Sigma_g^+/a^3\Pi_u)+C_2H_2(X^1\Sigma_g^+)$ reactions. *Chem. Phys. Lett.* **2003**, *382*, 112−119.

(37) Gu, X.; Guo, Y.; Zhang, F.; Mebel, A. M.; Kaiser, R. I. Reaction dynamics of carbon-bearing radicals in circumstellar envelopes of carbon stars. *Faraday Discuss.* **2006**, *133*, 245−275.

(38) Huang, L. C. L.; Balucani, N.; Lee, Y. T.; Kaiser, R. I.; Osamura, Y. Crossed beam reaction of the cyano radical, $CN(X^2\Sigma^+)$, with methylacetylene, CH_3CCH (X^1A_1): Observation of cyanopropyne, CH_3CCCN (X^1A_1), and cyanoallene, $H_2CCCHCN$ (X^1A'). *J. Chem. Phys.* **1999**, *111*, 2857−2860.

https://doi.org/10.1021/acs.jpca.2c08417
J. Phys. Chem. A 2023, 127, 1901−1908

(39) Kaiser, R. I. Experimental Investigation on the Formation of Carbon-Bearing Molecules in the Interstellar Medium via Neutral−Neutral Reactions. *Chem. Rev.* **2002**, *102*, 1309−1358.
(40) Becke, A. D. Density-functional thermochemistry. III. The role of exact exchange. *J. Chem. Phys.* **1993**, *98*, 5648−5652.
(41) Lee, C.; Yang, W.; Parr, R. G. Development of the Colle-Salvetti correlation-energy formula into a functional of the electron density. *Phys. Rev. B Condens. Matter* **1988**, *37*, 785−789.
(42) Knowles, P. J.; Hampel, C.; Werner, H. J. Coupled cluster theory for high spin, open shell reference wave functions. *J. Chem. Phys.* **1993**, *99*, 5219−5227.
(43) Purvis, G. D., III; Bartlett, R. J. A full coupled-cluster singles and doubles model: The inclusion of disconnected triples. *J. Chem. Phys.* **1982**, *76*, 1910−1918.
(44) Peterson, K. A.; Woon, D. E.; Dunning, T. H., Jr. Benchmark calculations with correlated molecular wave functions. IV. The classical barrier height of the $H+H_2 \rightarrow H_2+H$ reaction. *J. Chem. Phys.* **1994**, *100*, 7410−7415.
(45) Peterson, K. A.; Dunning, T. H. Intrinsic errors in several ab initio methods: The dissociation energy of N_2. *J. Phys. Chem.* **1995**, *99*, 3898−3901.
(46) Frisch, M. J.; Trucks, G. W.; Schlegel, H. B.; Scuseria, G. E.; Robb, M. A.; Cheeseman, J. R.; Scalmani, G.; Barone, V.; Petersson, G. A.; Nakatsuji, H.; et al. *Gaussian 16*, Revision B.01; Gaussian, Inc.: Wallingford, CT, 2016.
(47) Krajnovich, D.; Huisken, F.; Zhang, Z.; Shen, Y. R.; Lee, Y. T. Competition between atomic and molecular chlorine elimination in the infrared multiphoton dissociation of CF2Cl2. *J. Chem. Phys.* **1982**, *77*, 5977−5989.
(48) Gu, X.; Guo, Y.; Zhang, F.; Kaiser, R. I. Investigating the chemical dynamics of the reaction of ground-state carbon atoms with acetylene and its isotopomers. *J. Phys. Chem. A* **2007**, *111*, 2980−2992.
(49) Rettig, A.; Head-Gordon, M.; Doddipatla, S.; Yang, Z.; Kaiser, R. I. Crossed beam experiments and computational studies of pathways to the preparation of singlet ethynylsilylene (HCCSiH; X^1A'): The silacarbene counterpart of triplet propargylene (HCCCH; X^3B). *J. Phys. Chem. Lett.* **2021**, *12*, 10768−10776.
(50) He, C.; Fujioka, K.; Nikolayev, A. A.; Zhao, L.; Doddipatla, S.; Azyazov, V. N.; Mebel, A. M.; Sun, R.; Kaiser, R. I. A chemical dynamics study of the reaction of the methylidyne radical (CH, $X^2\Pi$) with dimethylacetylene (CH_3CCCH_3, X^1A_{1g}). *Phys. Chem. Chem. Phys.* **2022**, *24*, 578−593.
(51) Yang, T.; Bertels, L.; Dangi, B. B.; Li, X.; Head-Gordon, M.; Kaiser, R. I. Gas phase formation of c-SiC_3 molecules in the circumstellar envelope of carbon stars. *Proc. Natl. Acad. Sci. U.S.A.* **2019**, *116*, 14471−14478.

https://doi.org/10.1021/acs.jpca.2c08417
J. Phys. Chem. A 2023, 127, 1901−1908